

Identification of Alteration Zones with Using ASTER Data in A Part of Qom Province, Central Iran

Faranak Feizi*, Edris Mansuri

Department of Mining Engineering, South Tehran Branch, Islamic Azad University, Tehran, Iran

ABSTRACT

The main aim of this paper is utilizing the log-residual method (LRM) with the minimum noise fraction (MNF) transformation to create a pixel purity index (PPI) which was used to extract the most spectrally pure pixels from multispectral images in Kahak 1:25000 sheet, Central Iran. Spectral analyses of the clay minerals of the study area were obtained by matching the unknown spectra of the purest pixels to the U.S. Geological Survey (USGS) mineral library. Index minerals for alterations consisting of chlorite and epidote (for propylitic alteration), kaolinite, Halloysite, Dickite and montmorillonite (for argillic alteration), illite, muscovite, pyrite and Quartz (for phyllic alteration), goethite, hematite, jarosite and limonite (for Iron oxide zones) were identified by Spectral angle mapping (SAM) method in the area. In this paper, the various alteration zones were separated with using compositions of these all methods. These two alteration zones are important for porphyry copper deposits and gold mineralization in this area.

KEY WORDS: Log-residual method (LRM), Minimum noise fraction (MNF), Spectral angle mapping (SAM), Kahak, Iran

1. INTRODUCTION

The multispectral satellite images have widely application for mineral exploration due to presence of key minerals of alteration zones. Shortwave infrared (SWIR) bands from Advanced Space-borne Thermal Emission and Reflection Radiometer (ASTER) with the wavelength of ASTER SWIR bands between 1.65 and 2.43 μm has a good potential for mapping a hydrothermal alteration minerals such as pyrophyllite, kaolinite, illite-muscovite-sericite, and carbonate. In this range, hydroxide minerals which have been produced by hydrothermal alteration exhibit good absorption compared to shorter or longer wavelengths. Hunt & Salisbury, (1976).

The Advanced Space borne Thermal Emission and Reflection Radiometer (ASTER), which is aboard the Earth Observing System (EOS) TERRA platform, records solar radiation in 14 spectral bands (table 1). ASTER measures reflected radiation in three bands between 0.52 and 0.86 μm (VNIR) and in six bands from 1.6 to 2.43 μm (SWIR), with 15- and 30-m resolution, respectively Fujisada. (1995).

The VNIR, SWIR and TIR wavelength regions provide complementary data for lithological mapping. The three VNIR bands are important sources of information about absorption in transition metals, especially iron and some rare-earth elements (REE) Hunt, G. R., J. W. Salisbury, and C. J. Lenhoff (1974); Crowley, (1986), and for chlorophyll absorption in photosynthesizing vegetation. In the six SWIR bands carbonate, hydrate and hydroxide mineral spectra display molecular absorption features related to overtones and combination tones Hunt. (1977). This wavelength region has been exploited extensively for mineralogical mapping by using high-spectral-resolution imaging systems, such as the Air-borne Visible/Infrared Imaging Spectrometer (AVIRIS) Boardman, J. W., Kruse, F. A. (1994); Boardman, J. W., Kruse, F. A., Green. (1995). In this research, presence of Ba, Fe, Mn indexes in this area indicate the probability of presence the high potential areas for hydrothermal mineralization.

2. MATERIALS AND METHODS

2.1. Geological setting

The studied area is located between 50° 56' and 50° 59' longitude and 34° 19' and 34° 22' latitude in south of Qom province (Northeast of 1:100000 KAHAK Sheet). Based on 1:100000 geological map of Qom, the most impressive lithological features in studied area are the volcanic stones with basic combination. These features are included Andesite, Andesibasalt and megaporphyrite andesite. There are tuffaceous sandstone and limestones in east and southeast of investigated area. Ahadi & et al. (2010).

Hematization, limonitization, silicification and argillic alterations are seen in central parts that have been formed in north-south trend in east and northeast of studied area. Volcanic rocks have specific conditions. For example, ferrous

*Corresponding Author: Faranak Feizi, Department of Mining Engineering, South Tehran Branch, Islamic Azad University, Tehran, Iran, Tel: +982133722831 E-mail: feizi.faranak@yahoo.com

ore such as oligist formed along fracture in tectonic environment. Based on 1:100000 geological map of Kahak, three NE-SW faults have been seen. According to our results, around the faults, alteration and ferrous fluid have been observed (Fig. 1).

2.2. Data preprocessing

Data format (HDF) was used for this research. To remove atmospheric and topographic effects from ASTER SWIR and ASTER VNIR data, the log-residual method (LRM) Green, A. A., Berman, M., Switzer, B., & Craig, M. D. (1988) was used. The log-residual algorithm reduces noise from topography, instruments, and sun illumination, and was available as part of the analytical module used. The resulting data can be assumed to be more representative of the soils or lithologies of the exposed areas than the unprocessed data. Hence, a spectrum generated from data treated using the log-residual method will be more closely comparable to its corresponding library spectrum. Because the log-residual algorithm reduces noise from topography, instruments, and sun illumination, the processed ASTER SWIR and ASTER VNIR data will allow comparison of the synthesized spectrum with those from the library.

2.3. Data processing

Many image analysis and processing techniques can be used to interpret the spectral data. In this paper, several of these approaches are used, including the normalized difference vegetation index (NDVI), Optimum Index Factor (OIF), Minimum Noise Fraction (MNF), Spectral Angle Mapper (SAM), Principal component Analysis (PCA) and Pixel Purity Index (PPI) methods.

2.3.1. Optimum Index Factor (OIF) method

One of methods to find bands that participated to RGB is OIF index, would be preferred when they have higher index.

$$OIF = \frac{\sum_{i=1}^3 S_i}{\sum_{i=1}^3 |r_i|}$$

In this formula S_i is the standard Deviation of I band and r_i is the correlation coefficient between two bands of the tree bands combination. When they have higher index, color composite images derived from method is suitable for rock units descriptions. In this project, OIF index were processed for 84 different RGB. RGB that used for rock unit description can be seen as below:

RGB	4,6,9	4,8,9	4,6,8	4,5,9	4,5,6	4,5,8
OIF	8.695614	8.61291947	8.60824066	8.459765	8.39302513	8.360082

RGB 468 has higher OIF that can be used as guide in Aster data. Our surveys show this RGB is suitable for rock unit descriptions (Fig. 2).

2.3.2. Minimum noise fraction (MNF) method

MNF is a method similar to Principal Components used to segregate noise in the data, determine inherent data dimensionality, and reduce computational requirements for subsequent processing Green et al. (1988); Boardman and Kruse, (1994). For hyper spectral data (less-so for multispectral data), the MNF divides data space into two parts; one with large eigenvalues and coherent eigenimages and the second with near-unity eigenvalues and noise-dominated images. It is used as a preparatory transformation to put most of the interesting information into just a few spectral bands and to order those bands from most interesting to least interesting.

By applying these methods on VNIR and SWIR bands for ASTER, 9 bands created. By surveying of bands show MNF2 is suitable Propylitic alteration whit white color and Argillic alteration with black color. MNF4 is white for Argillic alteration (Fig. 3).

2.3.3. Pixel purity index (PPI) and n-D visualize method

The Pixel Purity Index (PPI) is used to find the most spectrally pure (extreme) pixels in multispectral and hyperspectral images Boardman and Kruse, (1994). These typically correspond to mixing end members. The PPI is computed by repeatedly projecting n-D scatter plots on a random unit vector. ENVI records the extreme pixels in each projection (those pixels that fall onto the ends of the unit vector) and it notes the total number of times each pixel is marked as extreme. A Pixel Purity Image is created where each pixel value corresponds to the number of times that pixel was recorded as extreme.

The PPI function can create a new output band or continue its iterations and add the results to an existing output band. The PPI is typically run on an MNF transform result, excluding the noise bands (see Minimum Noise Fraction Transform) Azizi & Mehrabi & Akbarpour, (2009). Whatever the iteration will be more, There would be better results in this method. the iteration is 20000 time in this project (fig.4). According to our diagram and images and comparing with classing that were used, we conclusion, in south and SE of studied area pure pixel were observed that would be suitable for alteration areas. With comparison to former methods or n-D visual and pixels classing can be determined alteration areas (Fig. 5).

After calculation of the PPI, the n-D visualizer was used in conjunction with the MNF and PPI results to locate, identify, and cluster the purest pixels and most extreme spectral responses in the data set. The n-D visualizer is an interactive tool for selection of the end members in n-space (Fig. 6).

With using this method, the especial pixels were classified and then these classes compared with the alteration minerals in USGS library. At last the alteration zones were distinguished.

2.3.4. Principal component Analysis (PCA) method

Use Principal Components to produce uncorrelated output bands, to segregate noise components, and to reduce the dimensionality of data sets. Because multispectral data bands are often highly correlated, the principal components (PC) transformation is used to produce uncorrelated output bands. This is done by finding a new set of orthogonal axes that have their origin at the data mean and that are rotated so the data variance is maximized Crosta & De Sousa & Azevedo & Brodie, (2003).

PC bands are linear combinations of the original spectral bands and are uncorrelated. You can calculate the same number of output PC bands as input spectral bands. The first PC band contains the largest percentage of data variance and the second PC band contains the second largest data variance, and so on. The last PC bands appear noisy because they contain very little variance, much of which is due to noise in the original spectral data. principal components bands produce more colorful color composite images than spectral color composite images because the data is uncorrelated. ENVI can complete forward and inverse PC rotations.

PC(1,4,5,7) were used for argillic alteration and static result show that pc4 should be inverse. PC(2,5,8,9) were used for epidote and static result show that pc2 should be normal. Finally, PC(2,5,8,9) were used for chlorite and static result show that pc4 should be inverse (epidote and chlorite show propylitic alteration) (Fig. 7).

2.3.5. Spectral Angle Mapper (SAM) method

Spectral Angle Mapper (SAM) is a physically-based spectral classification that uses an n-D angle to match pixels to reference spectra. The algorithm determines the spectral similarity between two spectra by calculating the angle between the spectra and treating them as vectors in a space with dimensionality equal to the number of bands. This technique, when used on calibrated reflectance data, is relatively insensitive to illumination and albedo effects. End member spectra used by SAM can come from ASCII files, spectral libraries, or you can extract them directly from an image (as ROI average spectra). SAM compares the angle between the end member spectrum vector and each pixel vector in n-D space. Smaller angles represent closer matches to the reference spectrum. Pixels further away than the specified maximum angle threshold in radians are not classified Kruse, (1988).

SAM classification assumes reflectance data. However, if you use radiance data, the error is generally not significant because the origin is still near zero.

Iron oxide zones were determined on VNIR bands. Mineral spectral such as Hematite, Goethite, Jarosite and limonite by aid of USGS were investigated (Fig. 8).

Argillic, Phyllic and Propylitic alterations were determined by aid of SWIR bands. Minerals spectral such as Kaolinite, Halloysite, Montmorillonite and Dickite were used for Argillic alteration (Fig. 9). Minerals spectral such as Chlorite and Epidote were used for Propylitic alteration (Fig. 10) and minerals spectral such as Illite, Moscovite, Pyrite and Quartz were used for phyllic alteration by aid of USGS library and alteration were determined (Fig. 11). these minerals are important in identification of hydrothermal alterations related to porphyry systems. Nouri, et al, (2012).

At last the final alteration map was prepared with integrating the different methods and alterations (Fig.12). finally the check filed process has done for confirming correction of the studies. These operations have shown the indicator minerals of oxidation zone in porphyry copper deposits. These observations are necessitate more research in southern part of the area (Fig.13a,b,c).

3. RESULT AND DISCUSSION

- Image processing with RGB:468 has shown The Propylitic alteration zone is located in southern part of the area and The Phyllic alteration zones are very poor in northwest and southwest.

- MNF method has shown that The Propylitic alteration zone is overlapping with previous method and The Argillic alteration zones are around the main drainage, northeast corner and a place near the central of the area.

- PPI method has completed the MNF and has separated Argillic and Propylitic alteration zones based on pure pixels.

- PCA method has shown Argillic alteration zones in northeast corner but it doesn't have shown the alteration around the main drainage and it was disseminated. Also this method confirmed the Propylitic alteration zone in south of the area.

- The processing with SAM method for Iron oxide zones has shown some disseminated places especially in south and southeast of the area. This method for The Argillic alteration zones has shown around the main drainage

,northeast corner and a place in northwest of the area . This method for The Propylitic alteration zones is overlapping with previous methods completely. Finally using this method for The Phallic alteration has shown a main place near the central parts and some other places like northeast south and southeast.

With comparing all above results and with taking into consideration the litho logical situation and overlapping the result of different methods we should choose the especial places with more overlapping for every alteration. Because all of the methods will not confirm each other and it is possible that some of them give the wrong results . So the Propylitic alteration zones were confirmed by every method such as RGB:468 and MNF and PPI and PCA and SAM. The Argillic alteration zones were confirmed by MNF(except the place near the central part)and PPI and PCA and SAM (except northwest) . The Phillic alteration zones with SAM has shown the main place in central part and south of the area which confirmed by check field and other places which were shown are false because of overlapping with the other alterations .

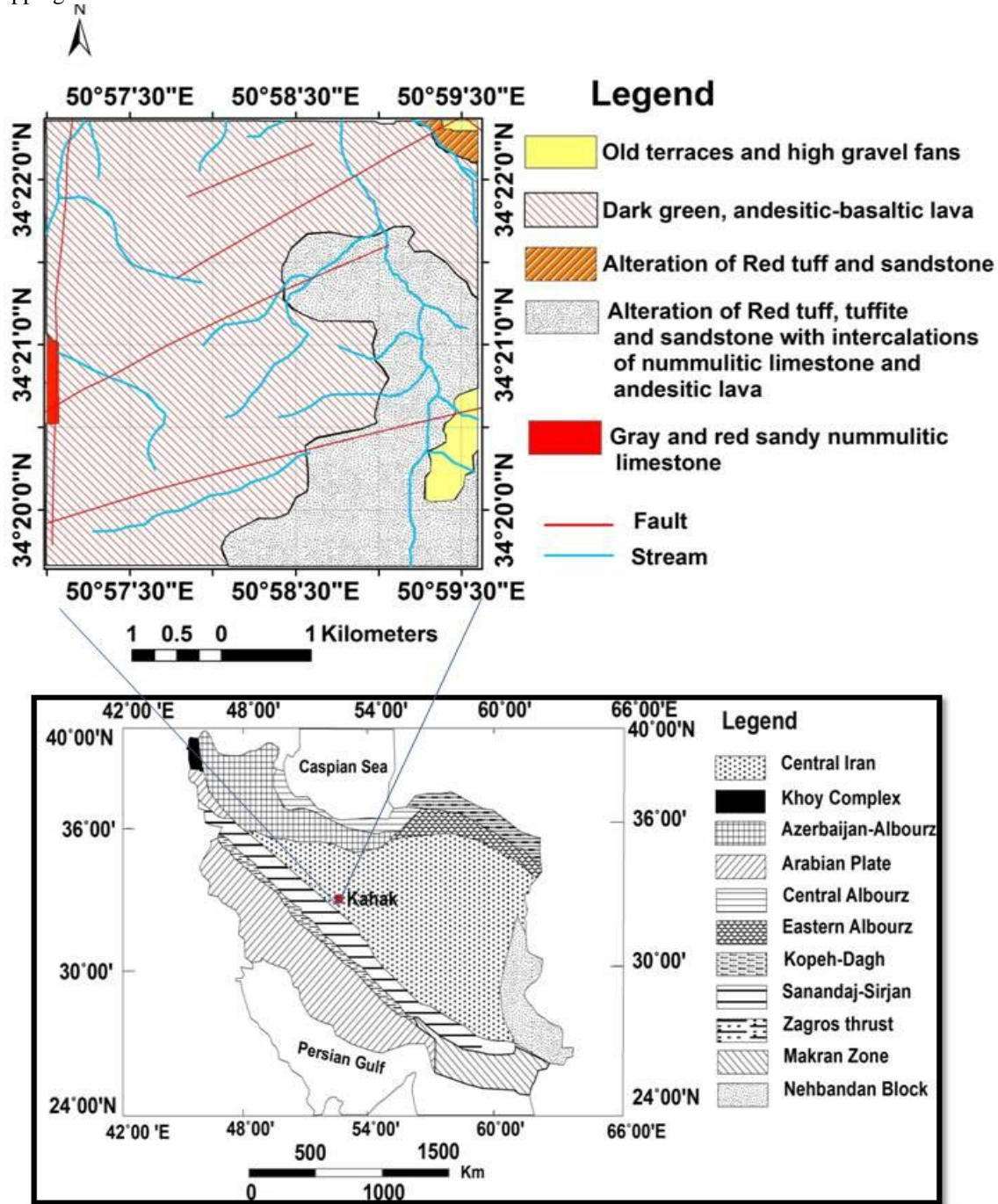


Fig. 1. tectonic map of Iran (Stocklin and Nabavi, 1972)(down), geology map of the Studied area (up)

Table 1: Performance parameters for the ASTER radiometer (Fujisada, 1995)

ASTER baseline performance requirements						
Subsystem	Band number	Spectral range (μm)	Radiometric resolution	Absolute accuracy (⊖)	Spatial resolution	Signal quantization levels
VNIR	1	0.52– 0.60	NEΔρ≤0.5%	≤±4%	15 m	8 bits
	2	0.63– 0.69				
	3N	0.78– 0.86				
	3B	0.78– 0.86				
SWIR	4	1.600– 1.700	NEΔρ≤0.5%	≤±4%	30 m	8 bits
	5	2.145– 2.185	NEΔρ≤1.3%			
	6	2.185– 2.225	NEΔρ≤1.3%			
	7	2.235– 2.285	NEΔρ≤1.3%			
	8	2.295– 2.365	NEΔρ≤1.0%			
	9	2.360– 2.430	NEΔρ≤1.3%			
	10	8.125– 8.475	NEΔT≤0.5K			
11	8.475– 8.825					
12	8.925– 9.275					
13	10.25– 10.95					
TIR	14	10.95– 11.65				
Stereobase-to-highest ratio	0.6 (along-track)					
Swath width	60 km					
Total coverage in cross-track direction by pointing	232 km					
Mission life	5 years					
MTF at Nyquist frequency	0.25 (cross-track) 0.20 (along-track)					
Band-to-band registration	Intra-telescope: 0.2 pixels Inter-telescope: 0.3 pixels of coarser band					
Peak data rate	89.2 Mbps					
Mass	406 kg					
Peak power	726 W					

Band number 3N refers to the nadir pointing view, whereas 3B designates the backward pointing view.

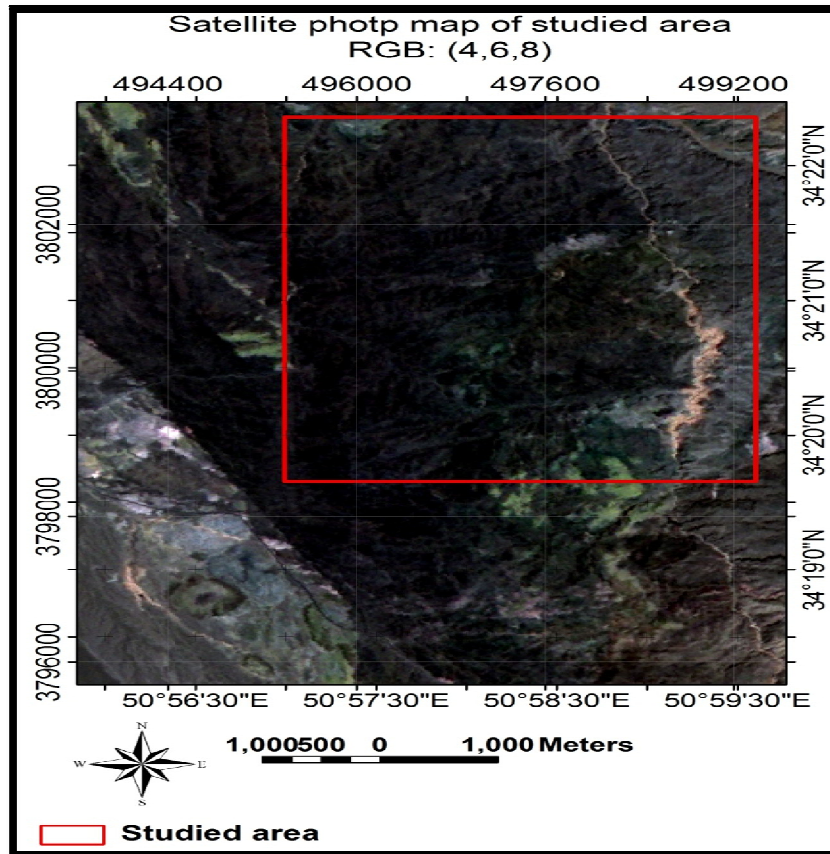


Fig.2. RGB (4,6,8): In this color composite, Propylitic alteration appears as green, and Phyllic alteration zones with large quantities of Al-OH minerals are pinkish to yellowish in color. (For interpretation of the references to color in this figure legend, the reader is referred to the web version of this article.)

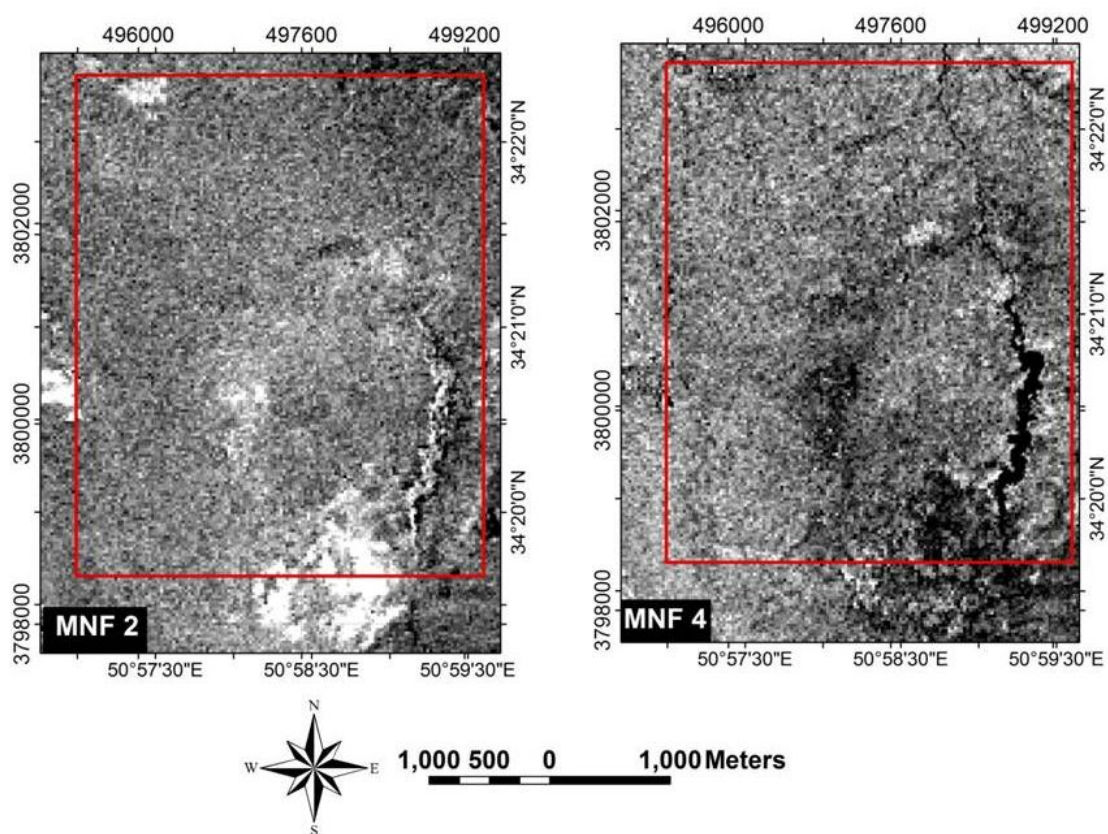


Fig. 3. MNF output bands. propylitic alteration appears as white in MNF2 and Argillic alteration appears as white in MNF4.

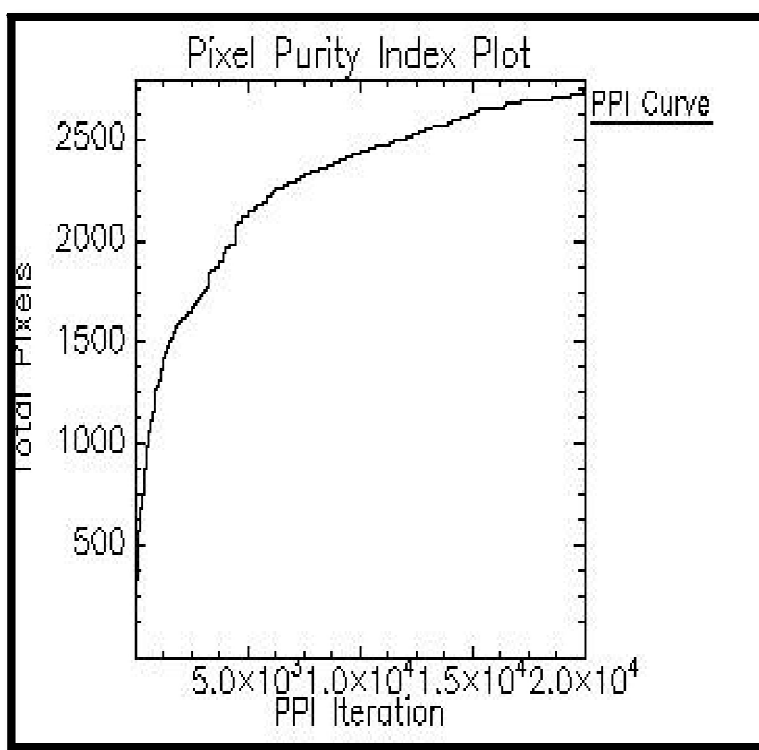


Fig.4. PPI plot with 20000 iteration

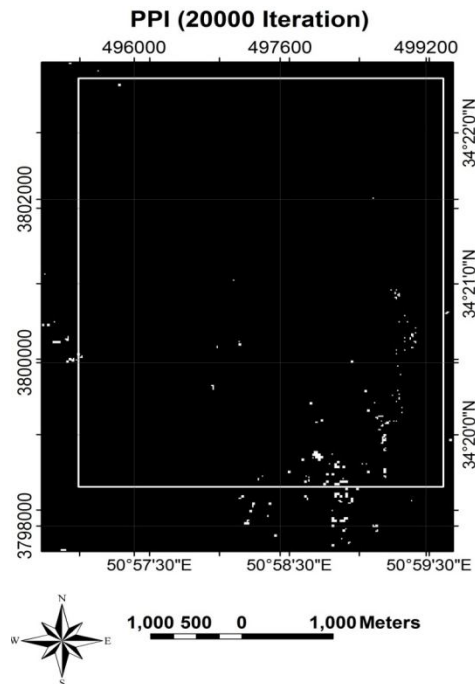


Fig.5.pure pixel were observed in white color especially in south of the area

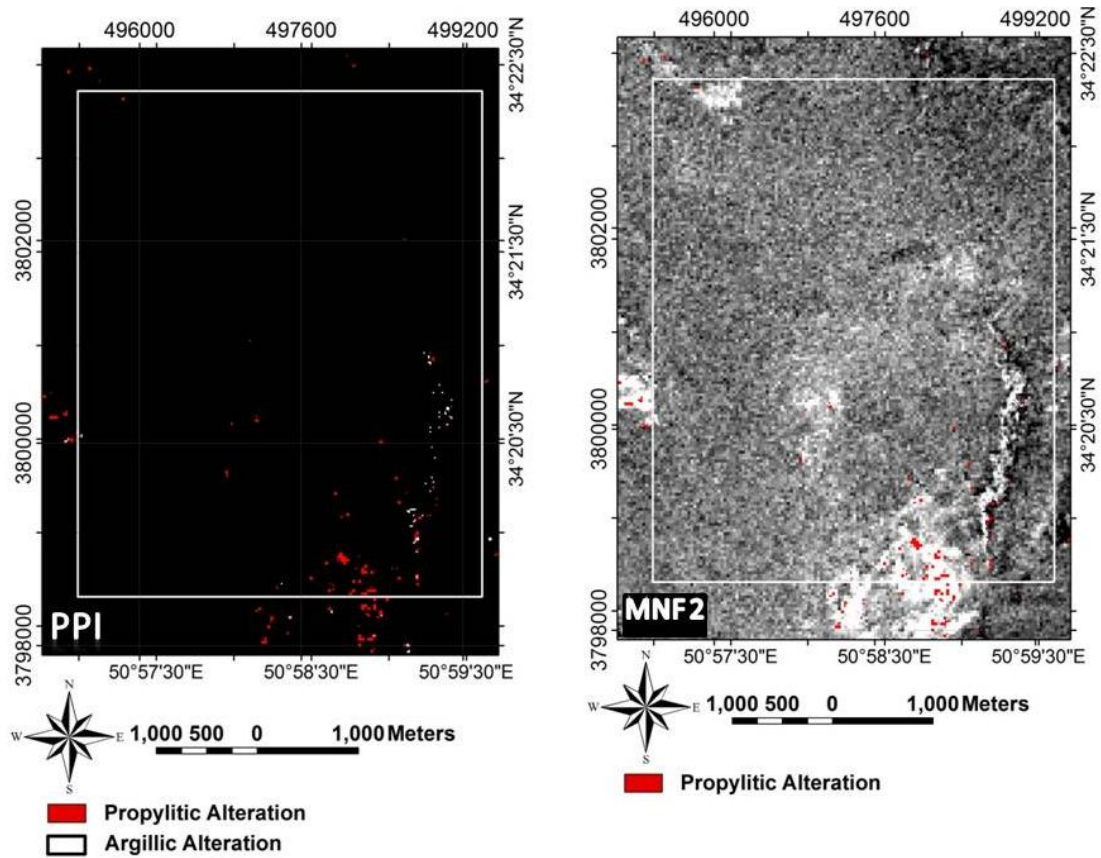


Fig. 6. in ppi image, red color alteration propylitic and white color show argillic alteration. On the left image can see, argillic and propylitic show accordance to each other.

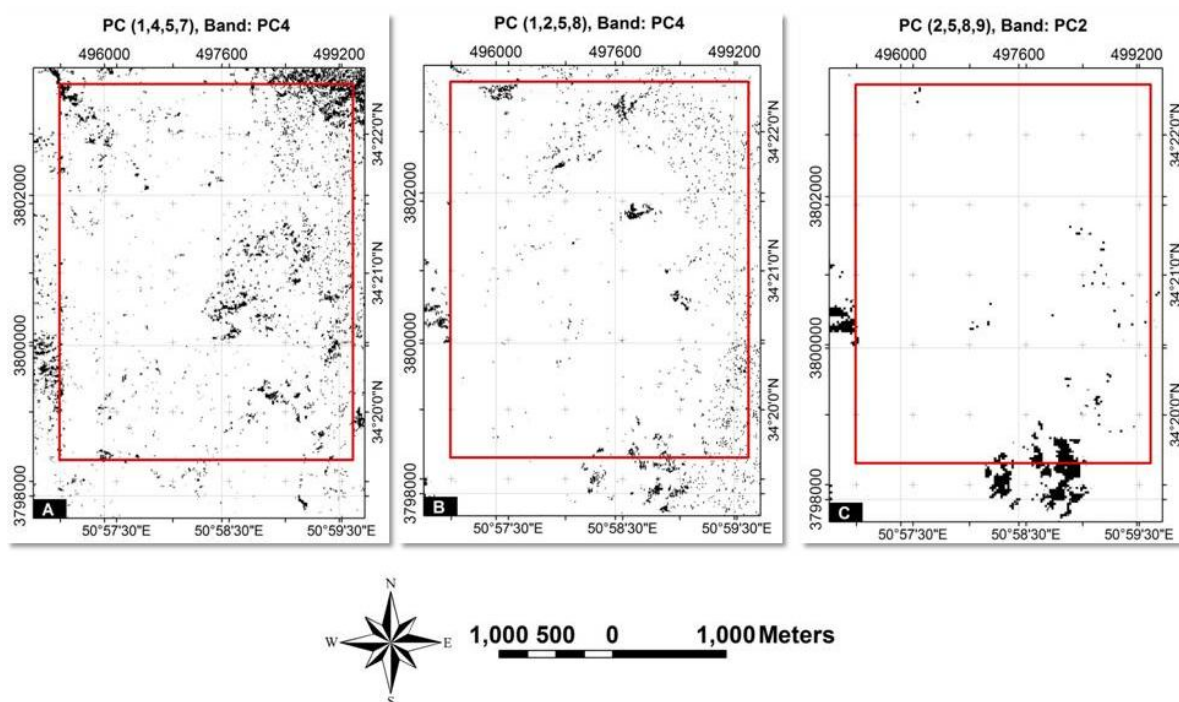


Fig.7. The images prepared based on PCA method , A:Argillic alteration , B:Epidote and C:chlorite

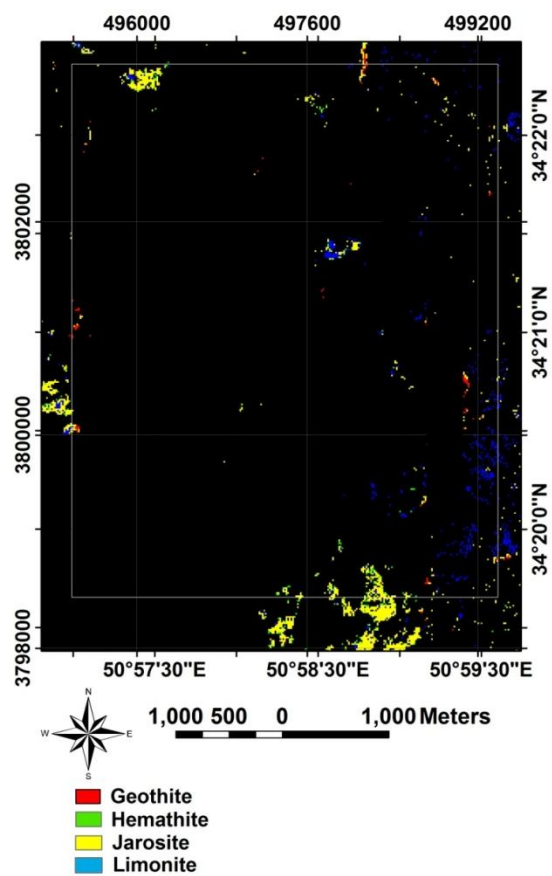


Fig.8. The image prepared based on SAM method for showing the Iron Oxide area

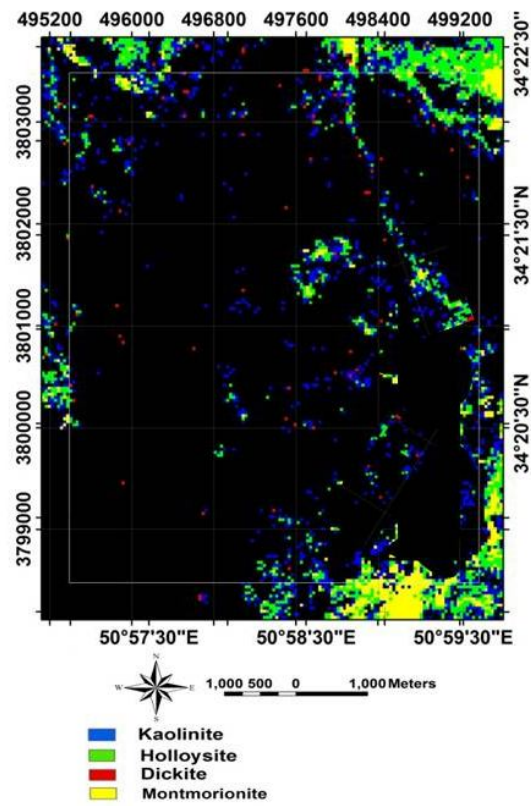


Fig.9. The image prepared based on SAM method for showing the Argillic alteration

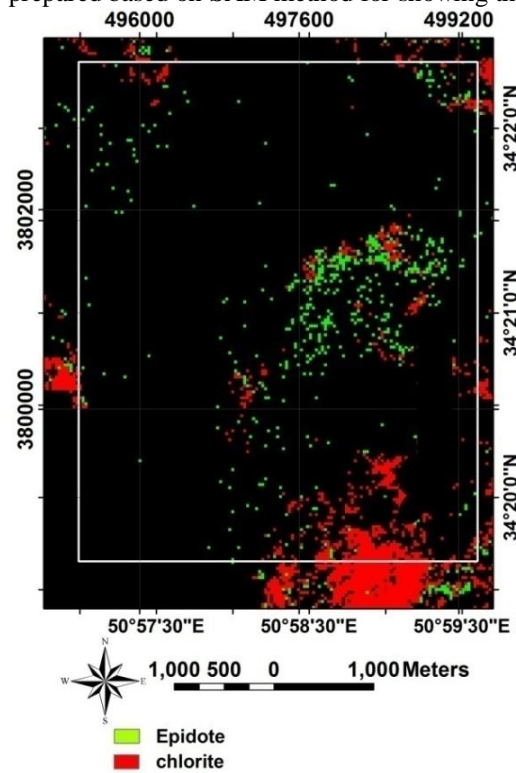


Fig.10. The image prepared based on SAM method for showing the Propylitic alteration

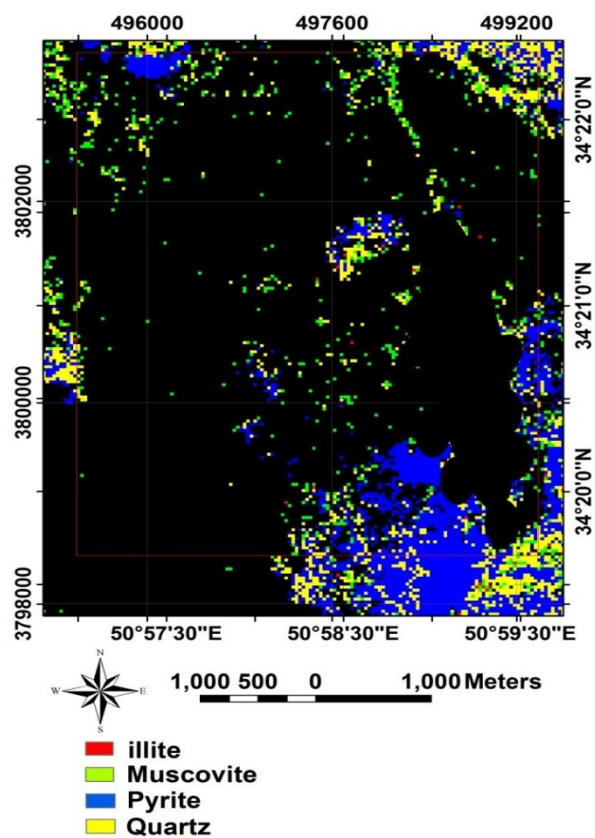


Fig.11. The image prepared based on SAM method for showing the Phyllic alteration

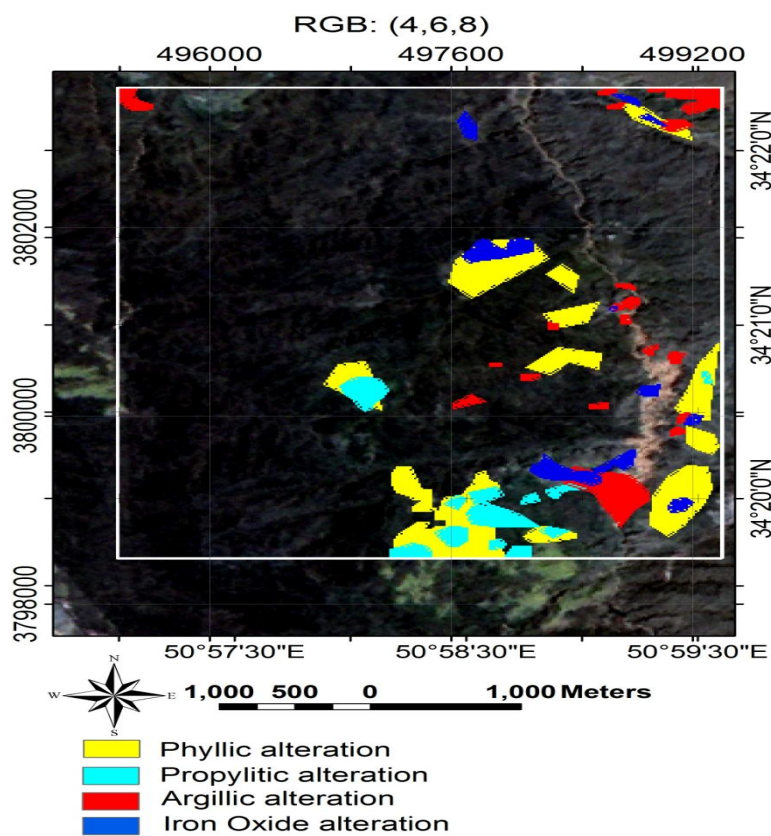


Fig. 12 . The final alteration map of the research area

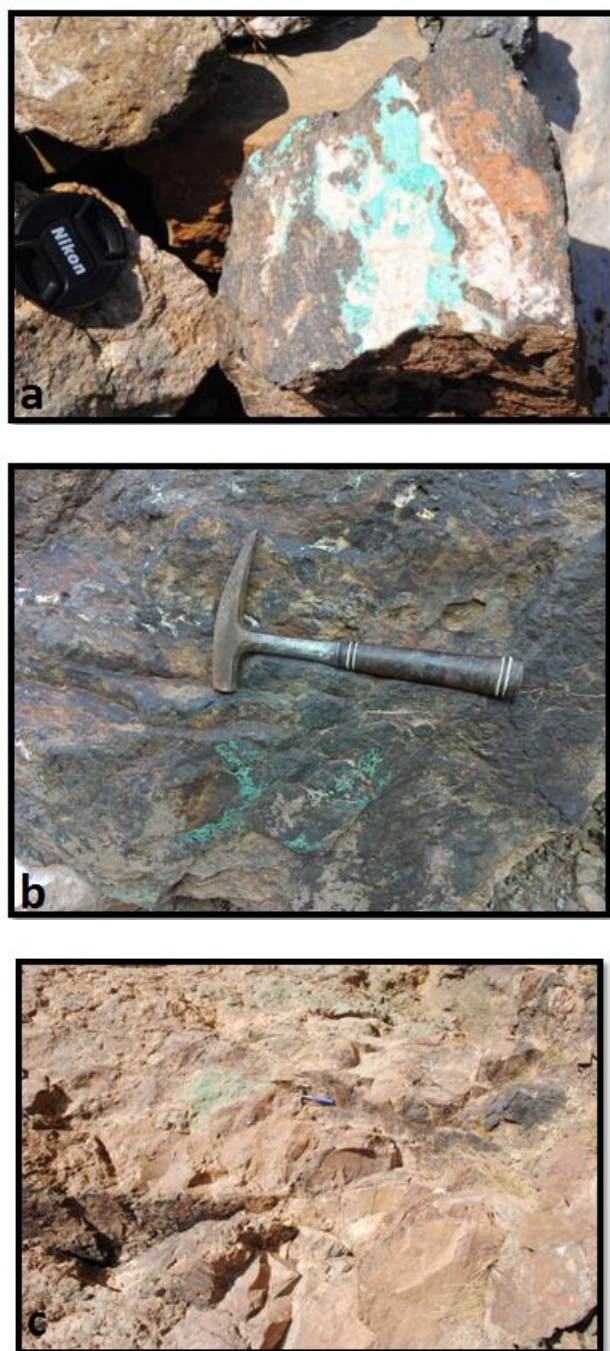


Fig.13. copper carbonates on surface of rocks are indicating the probability of copper porphyry deposit existence

4. Conclusions

The Argillic alteration is spreading in northeast and northwest corners and around the Veshnaveh stream. The Iron Oxide zone is spreading around the Veshnaveh stream. The Propylitic alteration is spreading in southern parts more than the others. The phyllic alteration is spreading around the Veshnaveh stream central and southern parts of the area.

The Argillic alteration has followed fault striking in main stream, so the suitable litho logy of tuffs will expand the Argillic alteration in this part. But this alteration doesn't have any mineral potentials, especially for Cu and Au.

The Propylitic and Phyllic alterations are existing in southern parts of the area and overlapping with a litho logy which is continuing to the outside of the research area.

The existence of these alterations , especially Quartz crystals with Pyrite (Phyllic alteration)are indicating the probability of presenting a porphyry system in southern parts .

REFERENCES

- Ahadi, GH., Kazem Zade, M., Seyed Hosseini, R. (2010). Geochemical prospecting in 1:25000 Kahak area(1:100000 Kahak geology sheet) , 170 page.
- Azizi, H., Mehrabi, B., Akbarpour, (2009). A. Genesis of tertiary magnetite apatite deposits, southeast of Zanjan, Iran. *Resour. Geol.* 59, 330–341.
- Boardman, J. W., & Kruse, F. A. (1994). Automated spectral analysis: a geologic example using AVIRIS data, north Grapevine Mountains, Nevada. *Proceedings of the Tenth Thematic Conference on Geologic Remote Sensing* (pp. I407 – I418). Ann Arbor: Environ. Res. Inst. Of Michigan.
- Boardman, J. W., Kruse, F. A., & Green, R. O. (1995). Mapping target signatures via partial un mixing of AVIRIS data. *Proceedings of the Fifth JPL Airborne Earth Science Workshop. JPL Publication*, vol. 95-01 (pp. 23–26). Pasadena, CA: Jet Propul. Lab.
- Crosta, A.P., De Sousa, F., Azevedo, C., Brodie, F. (2003). Targeting key alteration minerals in epithermal deposits in Patagonia, Argentina, using ASTER imagery and principal component analysis. *Int. J. Remote Sens.* 24, 4233–4240.
- Crowley, J. K., (1986). Visible and near-infrared spectra of carbonate rocks: Reflectance variations related to petrographic texture and impurities, *J. Geophys. Res.*, 91, No. B5, 5001-5012.
- Fujisada, H. (1995). Design and performance of ASTER instrument. *Proceedings of SPIE, the International Society for Optical Engineering*, 2583, 16– 25.
- Green, A. A., Berman, M., Switzer, B., & Craig, M. D. (1988). A transformation for ordering multispectral data in terms of image quality with implications for noise removal. *IEEE Transactions on Geoscience and Remote Sensing*, 26(1), 65– 74.
- Hunt, G. R.(1977). Spectral signatures of particulate minerals in the visible and near- infrared. *Geophysics*, 42, No. 3, 501-513.
- Hunt, G. R., and Salisbury, J. W.(1976). Visible and near-infrared spectra of minerals and rocks, XII. Metamorphic rocks, *Mod. Geol.*, 5, 219-228.
- Hunt, G. R., J. W. Salisbury, and C. J. Lenhoff , (1974). Visible and near-infrared spectra of minerals and rocks, X. Stony meteorites, *Mod. Geol.*, 5, 115-126.
- Kruse, F. A. (1988). Use of airborne imaging spectrometer data to map minerals associated with hydrothermally altered rocks in the northern Grapevine Mountains, Nevada–California. *Remote Sensing of Environment*, 24, 31– 52.
- Nouri, R. Jafari, M. Arain, M. and Feizi, F., (2012). Inter Relationship between Hydrothermal Alteration Zones and Lineaments in the Lohneh Area based on ASTER Data, Tarom Region, NW Iran. *Archives Des Sciences Journal*, 65